[1,2,3.]Victor Sunday AIGBODION

EXPERIMENTAL CORRELATION BETWEEN THE PROCESSING PARAMETER AND DIELECTRIC MATERIALS AND THERMAL CONDUCTIVITY OF EPOXY–CARBON NANOTUBE DECORATED WITH $CACO_3$ DERIVED FROM WASTE EGGSHELL

[1.]Africa Centre of Excellence, ACE–SPED University of Nigeria, Nsukka, NIGERIA
[2.]Department of Metallurgical and Materials Engineering, University of Nigeria, Nsukka, NIGERIA
[3.]Faculty of Engineering and Built Environment, University of Johannesburg, P. O. Box 534 Auckland Park, SOUTH AFRICA

Abstract: High thermal conductivity and dielectric materials with enhanced electrical conductivity are needed in advanced electronics. However, simultaneous improvement in this material remains a challenge. Here, the synergistic effect of dielectric materials and the high thermal conductivity of epoxy–carbon nanotube decorated with waste eggshell through the Taguchi–Grey experiment have been studied to achieve this challenge. The composite was produced by the solution stirring method. The dielectric constant, thermal and electrical conductivity, and morphology of the samples were evaluated. The optimal condition of the composite for higher electrical and thermal conductivity was obtained at 1wt%ESp, 2.5wt%CNTs, 90°C curing temperature, and 6 hours of curing time with 19,130% and 94.27% increments in thermal and electrical conductivity. The predicted grey relational grade was close to the experimental grey relational grade at a confidence limit of 95%. This validated the efficacy of the obtained optimal processing parameters. It was established that waste eggshells can be used to ensure good dispersion of CNTs for the production of conductive polymers for improved electrical and thermal conductivity.
Keywords: Electrical, thermal Conductivity, Waste eggshell, carbon nanotubes, Epoxy

1. INTRODUCTION

The low thermal conductivity of most polymer dielectrics has limited their widespread use in electronic devices, which is attributed to heat dissipation as a result of high speed, miniaturization of electronic devices, and high power [2–3]. The synergistic between dielectric materials and high thermal conductivity is one of the main limitations faced by scientists and engineers worldwide today. Research has shown that the addition of thermally conductive reinforcement can improve the dielectric materials and thermal conductivity of the composites [4]. The conductive reinforcements: graphite, carbon fibers, carbon black, metal fibers, metal powder, carbon nanotubes (CNTs), etc. have been reported as fillers for conductive polymer production [3, 4]. In all the mentioned conductive fillers, CNTs have exhibited fascinating usage in the production of conductive polymers [5].

Carbon nanotubes (CNTs) are normally produced from concentrically–rolled graphene sheets that have asymmetric helicity. The sp^2 of the carbon atoms of the CNTs provides high thermal conductivity and excellent high electronic and chemical stability [5]. The large aspect ratio, low mass density, and thermal properties of CNTs have increased their usage in the electronic industry. However, strong Van der Waals forces may occur due to the high dispersion of CNTs in the polymer as a result of segregation and agglomeration [6]. This results in a reduction in the mechanical properties and thermal and electrical conductivity. Hybridization of CNTs using inorganic materials helps to improve the mechanical and electrical properties of polymer composites. Also, the addition of CNTs to polymer leads to high hardness and embrittlement, which affects the polymer in areas where thermal conductivity is vital in the electronic industry [7].

Many scholars have used different inorganic fillers to decorate CNTs to improve the properties of polymer composites reinforced with CNTs. Among the works are Hao et al. [6] who used boron nitride nanosheets and silica to decorate CNTs for epoxy composites. They obtained 0.68Wm^{-1K-1}, which is 187% greater than that of epoxy. Aigbodion [7] synthesized green silver nanoparticles (AgNPs) to enhance the dielectric properties of carbon nanotubes (CNTs) and epoxy nanocomposites. They produced the composites using 0.5% AgNPs and 0.1, 0.2, 0.3, 0.4, and 0.5% CNTs in the epoxy matrix. They observed higher electrical conductivity at 0.5% AgNPs and 0.5% CNTs. Yang et al. [8] reported on coated MWCNTs with polypyrrole. They observed an increment in the dielectric constant and a decrease in the dielectric loss. Wang et al. [9] observed that the addition of diethylenetriamine and boron nitride nanosheets to functionalized MWCNTs results in low dielectric loss and high thermal conductivity. Salehi et al. [10] reported on the surface modification of carbon nanotubes (CNT) with HNO_3 and stearic acid (SA) on the morphological, thermal, and mechanical properties of nanocomposites using high–density polyethylene. The authors obtained incremental improvements in tensile strength and thermal properties.

Researchers have used $CaCO_3$ inorganic particles to enhance the dispersion of CNTs in the production of conductive polymers for the electrical and electronic industries. Shen and Zhu [11] reported on polyethylene (PE) matrix/carbon nanotubes (CNTs) decorated with $CaCO_3$. They observed higher electrical conductivity of

ISSN 1584 – 2665 (printed version); ISSN 2601 – 2332 (online); ISSN-L 1584 – 2665

the $CaCO_3$/PE composites at 0.5 wt% of CNTs. Backes et al. [1] reported on the use of montmorillonite, sepiolite, and calcium carbonate to decorate CNTs and epoxy composites. The authors obtained that the electrical conductivity of the composites rose due to the addition of calcium carbonate, while electrical conductivity was reduced with the addition of sepiolite. Li et al. [4] added $CaCO_3$ particles to develop polypropylene (PP)/CNT nanocomposites. They observed rises in electrical conductivity and a reduction in the percolation threshold of the nanocomposites. Md. Saleh et al. [12] developed calcium carbonate–filled CNT hybrid epoxy composites. They concluded that the transport properties of $CaCO_3$ act on CNTs and enhance good dispersion. From the literature, it was seen that $CaCO_3$ is a potential material for ensuring the dispersion of CNTs used in the production of conductive polymers. However, $CaCO_3$ is a major raw material used in the production of cement worldwide; this further increases the cost of producing conducting polymer. The need to source $CaCO_3$ from waste materials and reduce over–dependence on limestone for the decoration of CNTs for polymer composite production was the main focus of this work. Hence, this work aims to study the thermal and electrical conductivity of epoxy/CNTs using $CaCO_3$ derived from eggshell waste, since it has been reported by Hinckem [13] that eggshells contain 5 to 15% CaO. We expect that incorporating $CaCO_3$ from waste eggshell particles will not only enhance the dispersion of CNTs in the polymer but will enhance the electrical and thermal conductivity of the epoxy/CNT composites.

2. MATERIALS AND METHOD

— MATERIALS

The CNTs with 10–20m length and an average size of 10–40nm were sourced from Hongwu International China (Figure 1) and were used in this work. Epoxy LY556 of density 1.15–1.20g/cm^3 and hardener HY951 of density 0.98 g/cm^3 with structures displayed below in Figure 2 were used in this work. The brown eggshells were collected from the farm of the University of Nigeria, Nsukka, Nigeria.

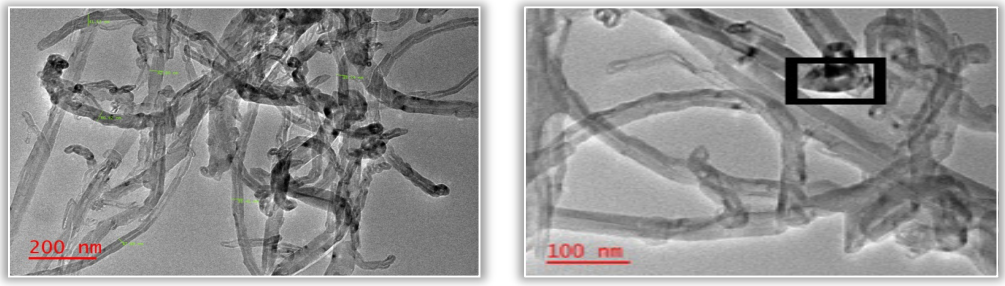

Figure 1: TEM image of CNTs

— METHODS

$CaCO_3$–ESp production

The collected brown eggshells were washed with water and dried for 24 hours to remove the membranes. A muffle furnace was used to calcine the cleaned eggshells to obtain $CaCO_3$. The furnace was operated at a temperature of 650 oC for five hours. Pulverization was done using a ball milling machine with 36 stainless steel balls and operating at a ball milling speed of 250rpm. The particle size analysis of the pulverized $CaCO_3$–ESp was done using a set of sieves and was sieved to a particle size of 65 m [13].

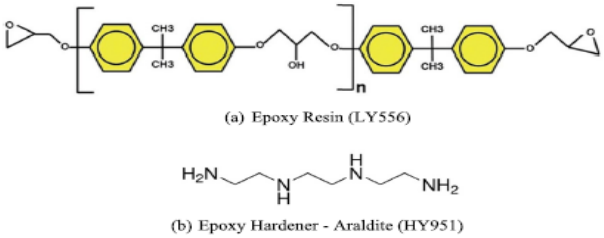

Figure 2: Structures of a) Epoxy resin b) Hardener

CNTs/$CaCO_3$–ESp Preparation

Before the decoration of CNTs with $CaCO_3$–ESp, the CNTs were modified by treating them with 100ml of 30% H_2O_2 and 65% HNO_3. The functionalized CNTs were mixed with $CaCO_3$–ESp using a sonicator Sonics ultrasonicated model. Vibra–Cell model VC 505 (solid probe) for 60 min at 400 W with an optimal addition of 0.5% $CaCO_3$–ESp was obtained in the formulation. The modified CNTs/CaCO3–ESp were used in the development of the novel composites.

Composites manufacturing

In the design of the experiment, the Taguchi–grey method (GRA) was used because the traditional Taguchi method is not able to solve the optimization of multi–objective. The orthogonal Taguchi technique was adopted in the design of the experiments, while grey analysis helps to combine the multiple responses into a single response. An L9 Taguchi design of experiments was used to evaluate the synergistic effect between dielectric materials and thermal and electrical conductivity.

ISSN 1584 – 2665 (printed version); ISSN 2601 – 2332 (online); ISSN-L 1584 – 2665

The processing parameters considered in this research were: wt%ESp (A), wt%CNTs (B), curing temperature (C), and curing time (D). The output parameters are dielectric materials and thermal and electrical conductivity. The dielectric materials and thermal and electrical conductivity were used for the optimization because of the relevance of these outputs to the electrical industry [7, 14]. The factors and the levels used in the work are shown in Table 1. This was made possible after preliminary experiments. Table 2 shows how the coding values were used to build the L9 orthogonal array.

Table 1: Factors and levels used in the work.

Process Parameters	Level 1(1)	Level 2(2)	Level 3(3)
Wt% Eggshell(ESp)	0	1	1.5
Wt% CNTs	0	2.0	2.5
Post Curing Temperature (°C)	60	90	120
Curing Time (Hours)	6	5	4

Table 2: Orthogonal array Taguchi Experimental Design layout.

S/No	%wtESp	%wtCNTs	Curing Temperature	Curing Time
1	1	1	1	1
2	1	2	2	2
3	1	3	3	3
4	2	1	2	3
5	2	2	3	1
6	2	3	1	2
7	3	1	3	2
8	3	2	1	3
9	3	3	2	1

The development of the novel composites was done using a modified solution stir–casting method. The epoxy resin and the hardener were used in the ratio of 10:1 and then stirred for 15 minutes using a magnetic stirrer. Air bubbles were eliminated using a roller press during the production of the composites. Table 2 was used in the formulation of the production of the composites. The composite mixture was cast in a pre–heated wooden mold and allowed for curing for 24 hours at room temperature. The yield of the combination of ESp (Wt %), CNTs (Wt %), post–curing temperature (°C), and curing time (hours) were considered as Taguchi array responses. The data was analyzed after conducting the electrical conductivity, dielectric materials, and thermal conductivity test experiments. The results were converted into S/N ratio values.

Composites Characterization

Joel's JEM–2100F model Transmission electron microscopy (TEM) was used to evaluate the microstructure of the CNTs/$CaCO_3$–ESp. Kaise insulation equipment (model SK5010) was used to determine the electrical conductivity of the samples as per ASTM by placing the samples between two electrodes. Equation 1 was used to compute the electrical conductivity. The thermal conductivity of the samples was determined using transient plane heat source techniques with model TPS2500s. Three readings were taken in each of the tests, and the average was used for the analysis.

$$\sigma = \frac{1}{\rho} = \frac{d}{(R_p)A} \tag{1}$$

Equation 2 was used to calculate the dielectric constant

$$\varepsilon^1 = \frac{C_P(A)}{A(\varepsilon_o)} \tag{2}$$

where: A=area, d = thickness, Cp= capacitance, β=electrical resistivity

VEGA 3 TESCAN model scanning electron microscope (SEM) was used to evaluate the microstructure of the composites. X'Pert Pro model diffractometer (XRD) was used to evaluate the phases.

3. RESULTS AND DISCUSSION

— Composition of the CaCO3–ESp

Table 3 shows the chemical analysis of the $CaCO_3$–ESp, it was observed that CaO has the main compound in $CaCO_3$–ESp with 85.68wt%. This weight percentage of CaO in the ESp confirmed that ESp contains mainly $CaCO_3$ and can be used in the replacement of $CaCO_3$ for the decoration of CNTs. The results of the $CaCO_3$–ESp obtained in this work are on par with Aigbodion and Akinlabi[15] and Hassan and Aigbodion [16].

Table 3: XRF analysis of $CaCO_3$–ESp

	%CaO	%Na_2O	%SiO_2	%Al_2O_3	%MgO	%MnO	%P_2O_5	%Fe_2O_3	%TiO_2	Loss of ignition
PWSnp	85.68	2.05	0.03	0.06	0.17	<0.01	0.85	0.08	0.01	5.47

— TEM images of CNTs and $CaCO_3$–ESp

Figure 3 displays the TEM images of the CNTs/$CaCO_3$–ESp. It was observed that there was a quiet difference in the TEM of the CNTs as shown in Figure 1 above. The decoration of the CNTs with $CaCO_3$–ESp greatly alters the multi–layer network arrangement of the CNTs. $CaCO_3$–ESp (black) was seen embedded in the CNTs. It was observed that there was little segregation obtained when CNTs were decorated with $CaCO_3$–ESp. This helps to ensure better distribution and dispersion of the CNTs in the polymer and increases the electronic pathways. This is inconsistent with the work of [17, 18].

ISSN 1584 – 2665 (printed version); ISSN 2601 – 2332 (online); ISSN-L 1584 – 2665

— Multi–response optimization

Table 4 displayed the results of the L9 Taguchi method multi–responses. Equation 3 was used to compute the grey relational generation (GRG) for higher the better from the ranges of 0 ≤ S/N ≤ 1

$$X_i(K) = \frac{X_i(K) - \min X(K)_i}{\max X - \min X_{I_i}(K)} \quad (3)$$

Equation 4 was used to compute the deviation sequence

$$\Delta_{0i}(k) = |x_0^{x}(k) - x_i^{x}(k)| \quad (4)$$

where k = 1 for i = 1 to 9. The grey relational generation and deviation results are given in Table 5

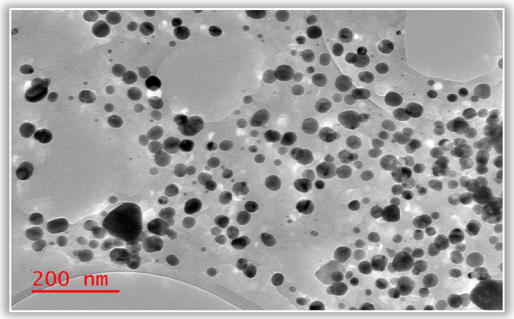

Figure 3: TEM image of CNTs–ESp

Table 4: Multi–responses results of the Taguchi experiment (L9)

S/No	%wtESp	%wtCNTs	Curing temperature	Curing time	Electrical conductivity (S/m)	Dielectric constant	Thermal conductivity $Wm^{-1}K^{-1}$
1	1	1	1	1	6.78E–09	4.35	0.65
2	1	2	2	2	7.81E–11	4.91	0.78
3	1	3	3	3	7.67E–12	4.56	0.98
4	2	1	2	3	6.52E–12	4.34	0.6
5	2	2	3	1	4.56E–09	4.67	0.65
6	2	3	1	2	1.54E–08	3.35	0.35
7	3	1	3	2	1.05E–08	2.22	0.88
8	3	2	1	3	1.34E–08	4.94	0.28
9	3	3	2	1	1.54E–09	4.81	0.34

The grey relational coefficients (GRC) was calculated from equation 5

$$\zeta_1(K) = \frac{\Delta_{mm} + \zeta\Delta_{max}}{\Delta_{0i}(k) + \zeta\Delta_{max}} \quad (5)$$

where: (Δoi(k) i,)= deviation from the normalized S/N value, Δmax (1)= maximum normalized S/N ratios, Δmin= minimum normalized S/N ratios, ξ= identification coefficient (0 ≤ ξ ≤ 1, and ξ equal = 0.5 was used.
Equation 6 was used to compute the Grey Relational Grade (GRG).

$$r_1 = \frac{1}{n}\sum_{k=1}^{n}\zeta_1(k) \quad (6)$$

where: Yi= GRG(nth experiment), n= number of performance features. The results of the GRC and GRG are given in Table 6.

Table 5: Deviation and Grey relational generation

S/NO	Grey relational generation			DOI		
	Electrical conductivity	Dielectric constant	Thermal conductivity	Electrical conductivity	Dielectric constant	Thermal conductivity)
1	0.440022659	0.783088235	0.528571429	0.559977341	0.216911765	0.471428571
2	0.004650021	0.988970588	0.714285714	0.995349979	0.011029412	0.285714286
3	7.4707E–05	0.860294118	1	0.999925293	0.139705882	0
4	0	0.779411765	0.457142857	1	0.220588235	0.542857143
5	0.295805757	0.900735294	0.528571429	0.704194243	0.099264706	0.471428571
6	1	0.415441176	0.1	0	0.584558824	0.9
7	0.681683414	0	0.857142857	0.318316586	1	0.142857143
8	0.870074863	1	0	0.129925137	0	1
9	0.0996188	0.952205882	0.085714286	0.9003812	0.047794118	0.914285714

Table 6: Grey Relational Grade (GRG) and Grey relational coefficient

S/NO	Grey relational coefficient			Grey Relational Grade (GRG
	Electrical conductivity	Dielectric constant	Thermal conductivity	
1	0.529988671	0.358456	0.485714286	0.458052946
2	0.74767499	0.255515	0.392857143	0.465348946
3	0.749962647	0.319853	0.25	0.439938529
4	0.75	0.360294	0.521428571	0.543907563
5	0.602097122	0.299632	0.485714286	0.462481253
6	0.25	0.542279	0.7	0.497426471
7	0.409158293	0.75	0.321428571	0.493528955
8	0.314962569	0.25	0.75	0.438320856
9	0.7001906	0.273897	0.707142857	0.560410172

ISSN 1584 – 2665 (printed version); ISSN 2601 – 2332 (online); ISSN-L 1584 – 2665

GRG evaluation

The GRG plot is shown in Figure 4; the midline represents the GRG's mean. All four variables in question were found to have abnormal patterns. The dielectric constant, thermal, and electrical conductivity are all affected by the wt percent ESp. Increasing the wt percent wt percent ESp from level 1(0) to level 2(1) raises grey relationship grades; however, increasing the wt percent ESp beyond level 2 lowers them. The weight percent of CNTs rose from level 1(0) to level 3 (2.5). The poor interfacial connection between the reinforcement and epoxy resin was blamed for the rise in GRG beyond level 1 (CNTs) and (ESP). A similar finding was made in the research of [19]. CNTs–ESp formed conductive network topologies and 3–D dense structures in the epoxy matrix, which resulted in a rise in the grey relational grade with increases in the wt percent CNTs at level 2 and ESp at level 3. Charge carriers in the system move quickly the conductive channels in the epoxy matrix. Ohmic and non–ohmic conduction came from direct contact of CNTs–ESp in the epoxy, resulting in indirect contact of CNTs–ESp in the matrix [20].

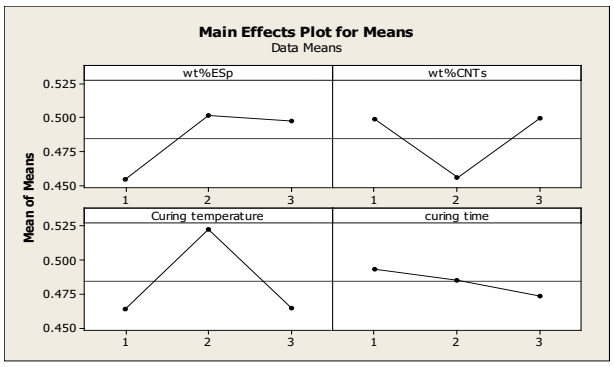

Figure 4: Grey relational grade diagram for the multi–response

The curing temperature increases the GRG from level 1 (60°C) to level 2 (90°C), while the curing time reduces from level 1 (6 hrs) to level 3 (4 hrs). This was attributed to the thermal stability and setting of the composites that occurred during thermal curing [21]. However, a thermal curing temperature of 90°C and a decrease in curing time raise the dielectric constant and thermal and electrical conductivity. The reduction of GRG as the curing time rises to level 3 leads to prolonging the time of curing, hence decreasing the interfacial bonding between the reinforcement and epoxy [21].

Analysis of Response Surfaces

Analysis of surface response was further used to discuss the effect of the GRG on the four factors. Figure 5 displays the various plots of the surface response obtained in this work. This was made possible using Minitab16.

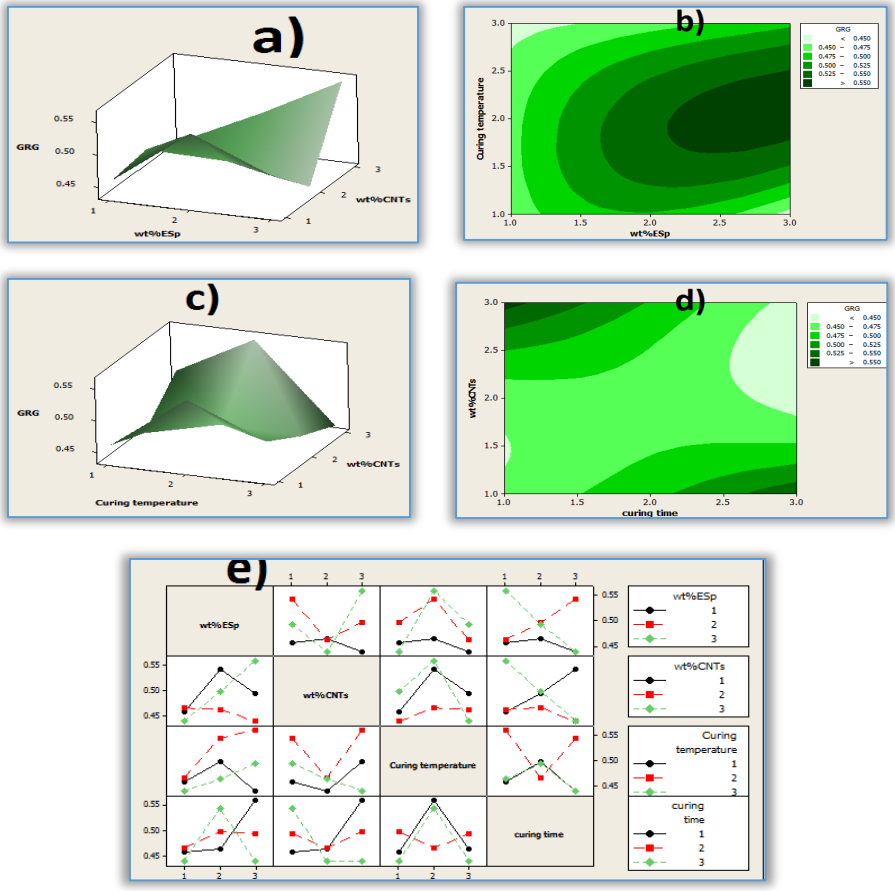

Figure 5: Response plots of a) GRG with wt%CNTs and wt%ESp b) GRG with wt%ESp and curing temperature c) GRG with wt%CNTs and curing temperature d) GRG with wt%CNTs and curing time d) interaction plots of all the factors

ISSN 1584 – 2665 (printed version); ISSN 2601 – 2332 (online); ISSN-L 1584 – 2665

It is clear in Figure 5a–5b that increasing wt%ESp from level 1 to level 3 slightly reduces GRG, A higher amount of wt%ESp beyond the optimum may not have any positives. This is inconsistent with the works of [18, 21]. It was observed from Figure 5c–5d that the reduction of the dielectric constant and thermal and electrical conductivity were obtained at a minimum level of wt%CNTs. The greater effect of curing time and temperature was noticeable in Figure 5. The maximum level of the ESp and CNTs helps to raise the thermal and electrical conductivity. The interaction plot in Figure 5d represents the synergistic influences of the four factors on the dielectric constant, thermal and electrical conductivity. It was observed that the maximum values of the dielectric constant and thermal and electrical conductivity were obtained at levels 2 and 3 for ESp (1 wt%), level 2 for CNTs (2.5 wt%), level 2 for curing temperature (90°C), and level 1 for curing time (6 hrs).

GRG Optimal Setting

Table 7 shows the mean to mean values of the GRG. The curing temperature has a higher delta value of 0.0586, ranked 1 with a higher value at level 2 (0.5232), followed by wt%ESp with delta values of 0.0468, ranked 2 with a higher setting at level 2 (0.5013), then wt% CNTs with delta values of 0.0439, ranked 3 with a greater point at level 3 (0.4993), and the least was curing time, ranked 4 with delta values of 0.0441 and optimal setting at level 1 (0.4936). Hence the greater effect on dielectric constant, thermal and electrical conductivity for high electrical and thermal conductivity according to the ranking follows: curing temperature wt%ESp wt%CNTs curing time. The optimal settings for this present work are wt%ESp (level 2), curing temperature (level 2), wt%CNTs (level 3), and curing time (level 1) (Table 8). As a result, the optimal conditions are as follows: 1wt%ESp, 90oC curing temperature, 2.5wt%CNTs, and 6 hours curing time.

Table 7: Means Response Table for GRG (Mean of GRG value= 0.4844)

Level	%wtESp(A)	%wt CNTs (B)	Curing temperature©	Curing time(D)
1	0.4544	0.4985	0.4646	0.4936
2	0.5013	0.4554	0.5232	0.4854
3	0.4974	0.4993	0.4653	0.4741
Delta	0.0468	0.0439	0.0586	0.4741
Rank	2	3	1	4

The predicated optimal condition of the GRG value is given in equation 7.

$$\text{Predicated GRG} = 0.4844+(0.5013-0.4844)+(0.4993-0.4844)+(0.4646-0.4844)+(0.4936-0.4844) \quad (7)$$

$$\text{Predicated GRG} = 0.4844+0.0169+0.0149-0.0198+0.0092$$

$$\text{Predicated GRG} = 0.5056$$

Table 8: Process Parameters and their optimum level

Process factors	Designation	Optimum level	GRG	
Wt%ESp	A	L2 (1wt %)	Prediction 0.5056	Experiment 0.560
Wt%CNTs	B	L3 (2.5wt %)		
Curing temperature	C	L2 (90°C)		
Curing Time	D	L1 (6hours)		

An experiment was conducted using the optimal conditions, and the values obtained for the four factors are dielectric constants (4.25), electrical conductivity (1.25×10^{-9}S/m), and thermal conductivity (0.75 $Wm^{-1}K^{-1}$). The values obtained for the optimal condition are within the acceptable limit for microelectronic devices [5, 6]. The enhanced thermal conductivity was attributed to a reduction in the interfacial thermal barrier between the CNTs–$CaCO_3$–ESp and the epoxy in the composites. A good synergetic effect between CNTs–$CaCO_3$–ESp and the epoxy at the optimal position improved electrical and thermal conductivity since the computed value GRG was 0.5056 and the experimental values 0.560. Hence, the predicted optimal GRG of 0.5056 is within the 95% confidence limit of 0.560 experimental GRG. This validated the efficacy of the obtained optimal processing parameters.

— XRD examination

The various phases formed were analyzed using XRD. Figure 6 shows the results of the XRD analysis. It was seen that the epoxy has amorphous phases. This phase of the epoxy was on par with the work of [5]. The CNTs have a crystalline phase of 100, 102, and 110. These phases are associated with C (carbon) and C6O (carbon). These crystalline phases observed in the CNTs were inconsistent with the findings of [5]. The XRD patterns of the ESp revealed phases of (111), (200), (220), and (111) respectively. The phases of the ESp were associated with CaO and $CaCO_3$. Evidence of CNTs and ESp was visible in the composite. The addition of the CNTs and ESp alters the amorphous phase's nature of the epoxy to the crystalline–amorphous phase. The CNTs were strongly attached to the ESp, as evidenced in the XRD spectrum of the composite. The crystalline size of the samples under investigation was determined using equation 8. The crystalline sizes of 34.56, 25.78, 10.67, and 8.90 nm were obtained for the epoxy, composite, CNTs, and ESp, respectively. The ESp has the highest crystalline size of all

ISSN 1584 – 2665 (printed version); ISSN 2601 – 2332 (online); ISSN-L 1584 – 2665

the samples. The presence of ESp–CNTs in the epoxy may increase the electron path of the polymer and make the polymer semi–conductive [18].

$$D = \frac{0.9\lambda}{\beta Cos\theta} \tag{8}$$

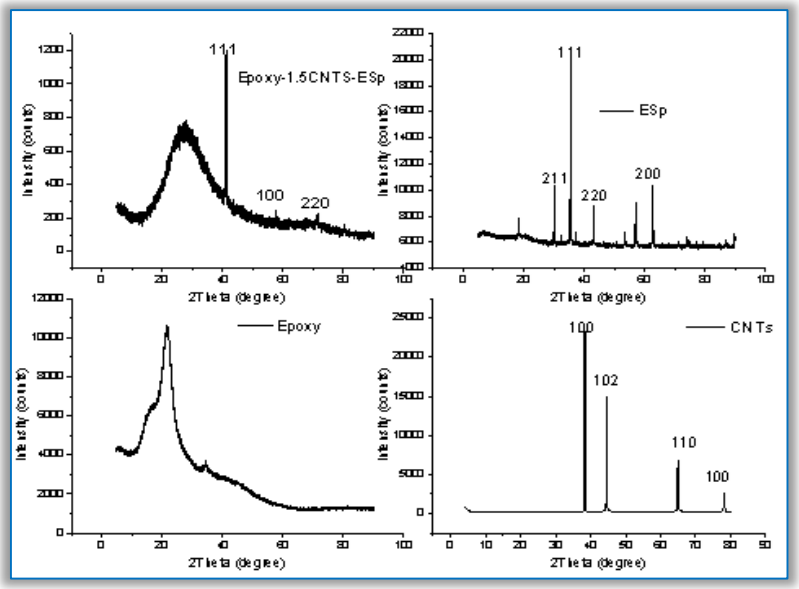

Figure 6: XRD spectrum of the samples

— SEM Evaluation

The SEM image is displayed in Figure 7. There was a significant difference between the SEM images of epoxy as compared with that of the composites. The reinforcement is prominently displayed as white phases. The presence of these white phases of CNTs increases as the number of CNTs rises to 2wt%CNTs and 1wt%ESp. A uniform and good distribution of ESp was obtained in the decorated sample with 1wt%ESp. The presence of ESp helps to alter the network multilayer structure of CNTs and enhances good bonding between the reinforcement and polymer (Figure 7b). This enhances interfacial bonding and has been previously reported in [11, 12] when using $CaCO_3$ from limestone. Small agglomerates and segregation CNTs were obtained in the samples as the percentage of ESp rose to 1.5wt% (Figure 7c). As shown in Figures 4 and 5, when these CNTs stick together, they may lose some of their ability to conduct electricity.

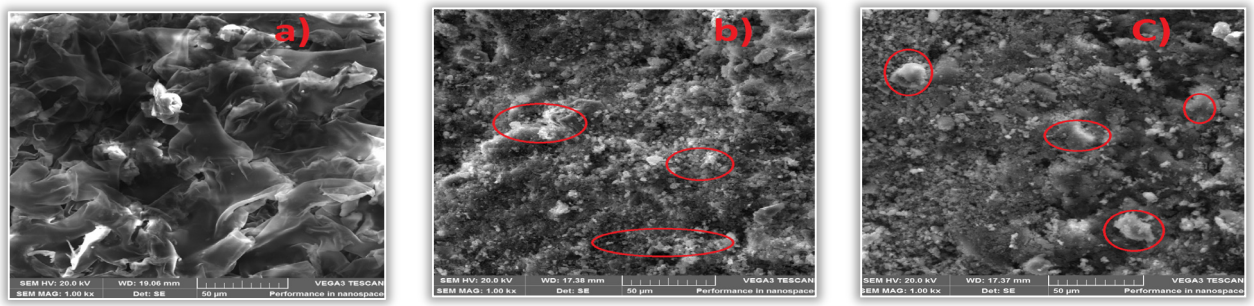

Figure 7: SEM images of a) Epoxy b) 1wt%ESp–2.5wt%CNTs/Epoxy C) 1.5wt%ESp–2.5wt%CNTs/Epoxy

4. CONCLUSIONS

New insights into the synergistic effect of dielectric materials and the high thermal conductivity of epoxy–Carbon nanotube decorated with waste eggshell via the Taguchi–Grey experiment have been studied. The optimal composite condition was determined to be 1 wt%ESp, 2.5 wt%CNTs, 90°C curing temperature, and a 6–hour curing time. The high electrical and thermal conductivity and dielectric constant obtained under optimal conditions were attributed to the high electron mobility of ESp–CNTs, which helps to enhance the conductivity of the epoxy. The predicted optimal GRG of 0.5056 is within the 95% confidence limit of 0.560 experimental GRG. This validated the efficacy of the obtained optimal processing parameters. The dielectric constants (4.25), electrical conductivity ($1.25x10^{-9}$S/m) and thermal conductivity (0.75 $Wm–1K^{-1}$) are all known. The values obtained for the optimal condition are within the acceptable limit for microelectronic devices. It was established that waste eggshells can be used to ensure good dispersion of CNTs for the production of conductive polymers.

ISSN 1584 – 2665 (printed version); ISSN 2601 – 2332 (online); ISSN-L 1584 – 2665

Acknowledgement

The authors appreciate the Africa Centre of Excellence for Sustainable Power and Energy Development, ACE–SPED, University of Nigeria, Nsukka, Faculty of Engineering and Built Environment, University of Johannesburg, Auckland Park, South Africa, for their support.

References

[1] Backes, E. H., Sene, T. S., Passador, F. R., Pessan, L. A. (2017). Electrical, Thermal and Mechanical Properties of Epoxy/CNT/Calcium Carbonate Nanocomposites. Materials Research, 21(1)
[2] Backes, E. H., Passador, F. R., Leopold, C., Fiedler, B., Pessan, L. A. (2018). Electrical, thermal and thermo–mechanical properties of epoxy/multi–wall carbon nanotubes/mineral fillers nanocomposites. Journal of Composite Materials, 002199831876349
[3] Md Saleh, S. S., Suhaimi, S. M., Md Akil, H., Mohammad, N. F. (2020). Properties of Carbon Nanotubes–Calcium Carbonate Hybrid Filled Epoxy Composites. Materials Science Forum, 1010, 136–141
[4] Li, X.–H., He, Y., Li, X., An, F., Yang, D., Yu, Z.–Z. (2017). Simultaneous Enhancements in Toughness and Electrical Conductivity of Polypropylene/Carbon Nanotube Nanocomposites by Incorporation of Electrically Inert Calcium Carbonate Nanoparticles. Industrial & Engineering Chemistry Research, 56(10), 2783–2788
[5] Rudawska, A. (2020). Experimental Study of Mechanical Properties of Epoxy Compounds Modified with Calcium Carbonate and Carbon after Hygrothermal Exposure. Materials, 13(23), 5439
[6] Hao, Y.; Li, Q.; Pang, X.; Gong, B.; Wei, C.; Ren, J. Synergistic Enhanced Thermal Conductivity andDielectric Constant of Epoxy Composites with Mesoporous Silica Coated Carbon Nanotube and Boron Nitride Nanosheet. Materials 2021, 14, 5251
[7] Victor S. Aigbodion (2021) Explicit microstructure and electrical conductivity of epoxy/carbon nanotube and green silver nanoparticle enhanced hybrid dielectric composites, Nanocomposites, 7:1, 35–43
[8] Yang, C.; Lin, Y.; Nan, C.W. Modified carbon nanotube composites with high dielectric constant, low dielectric loss and large energy density. Carbon 2009, 47, 1096–1101.
[9] Wang, Y.; Hou, Y.; Deng, Y. Effects of interfaces between adjacent layers on breakdown strength and energy density in sandwichstructured polymer composites. Compos. Sci. Technol. 2017, 145, 71–77.
[10] Salehi, S., Maghmoomi, F., Sahebian, S., Zebarjad, S., Lazzeri, A. (2019). A study on the effect of carbon nanotube surface modification on mechanical and thermal properties of CNT/HDPE nanocomposite. Journal of Thermoplastic Composite Materials, 089270571983800
[11] Shen, W., & Zhu, A. (2021). Sub-micron calcium carbonate isolated carbon nanotubes/polyethylene composites with controllable electrical conductivity. Journal of Applied Polymer Science, 138(47), 51412. Portico.
[12] Md Saleh, S. S., Suhaimi, S. M., Md Akil, H., Mohammad, N. F. (2020). Properties of Carbon Nanotubes–Calcium Carbonate Hybrid Filled Epoxy Composites. Materials Science Forum, 1010, 136–141
[13] Hincke Maxwell T., Yves Nys, Joel Gautron, Karlheinz Mann, Alejandro B. Rodriguez–Navarro, Marc D. McKee (2012). The eggshell: structure, composition and mineralization. Frontiers in Bioscience, 17(1), 1266
[14] Zhang, C.; Xiang, J.; Wang, S.; Yan, Z.; Cheng, Z.; Fu, H.; Li, J. Simultaneously Enhanced Thermal Conductivity and Breakdown Performance of Micro/Nano–BN Co–Doped Epoxy Composites. Materials 2021, 14, 3521. [CrossRef]
[15] Aigbodion V.S., Akinlabi E.T., 2019 Explicit microstructural evolution and electrochemical performance of zinc eggshell particles composite coating on mild steel, Surf. and Interf. 17, 100387
[16] Hassan S.B. and Aigbodion V.S, 2015. Effects of eggshell on the microstructures and properties of Al–Cu–Mg/eggshell particulate composites, J. of King Saud Univer. – Eng. Sci., 27, 49–56
[17] Jin, F.–L., Park, S.–J. (2013). Recent Advances in Carbon–Nanotube–Based Epoxy Composites. Carbon Letters, 14(1), 1–13
[18] Zhang, D.–L.; Zha, J.–W.; Li, C.–Q.; Li, W.–K.; Wang, S.–J.; Wen, Y.; Dang, Z.–M. High thermal conductivity and excellent electrical insulation performance in double–percolated three–phase polymer nanocomposites. Compos. Sci. Technol. 2017, 144, 36–42. [CrossRef]
[19] Liu, C.; Li, M.; Shen, Q.; Chen, H. Preparation and Tribological Properties of Modified MoS2/SiC/Epoxy Composites. Materials 2021, 14, 1731. [CrossRef] [PubMed]
[20] Smolen, P.; Czujko, T.; Komorek, Z.; Grochala, D.; Rutkowska, A.; Osiewicz–Powezka, M. Mechanical and Electrical Properties of Epoxy Composites Modified by Functionalized Multiwalled Carbon Nanotubes. Materials 2021, 14, 3325. [CrossRef]
[21] Kopparthi, P. K., Kundavarapu, V. R., Kaki, V. R., Pathakokila, B. R. (2020). Modeling and multi response optimization of mechanical properties for E–glass/polyester composite using Taguchi–grey relational analysis. Proceedings of the Institution of Mechanical Engineers, Part E: Journal of Process Mechanical Engineering, 095440892096259

ISSN 1584 – 2665 (printed version); ISSN 2601 – 2332 (online); ISSN-L 1584 – 2665